JEE Journal of Ecological Engineering

Journal of Ecological Engineering 2022, 23(10), 291–303
https://doi.org/10.12911/22998993/152524
ISSN 2299–8993, License CC-BY 4.0

Received: 2022.07.17
Accepted: 2022.08.22
Published: 2022.09.01

Treatment of Petroleum Refinery Wastewater by Graphite–Graphite Electro Fenton System Using Batch Recirculation Electrochemical Reactor

Ali Nadhum Kassob[1*], Ali Hussein Abbar[2]

[1] Chemical Engineering Department, University of Al-Qadisiyah, Al-Qdisiyyah, 58002, Iraq

[2] Department of Biochemical Engineering, Al-Khwarizmi College of Engineering, University of Baghdad, Baghdad, 10071, Iraq

* Corresponding author's e-mail: alinadhum9595@gmail.com

ABSTRACT

Water pollution and the lack of access to clean water are general global problems that result from the expansion of industrial and agricultural activities. Petroleum refinery wastewaters are considered as a major challenge to the environment and their treatment is mandatory. The present work investigated the removal of chemical oxygen demand (COD) from petroleum refinery effluents generated from the Al-Dewaniya petroleum refinery plant located in Iraq by utilizing a novel graphite–graphite electro-Fenton (EF) system. The electrochemical reactor was a tubular type with a cylindrical cathode made from porous graphite and concentric porous graphite rode acts as an anode. By adopting the response surface methodology (RSM), the impacts of different operating variables on the COD removal were investigated. The optimal conditions were a current density of 25 mA/cm^2, $FeSO_4$ concentration of 1.4 mM, and electrolysis time of 90 minutes, which resulted in the COD removal efficiency (RE%) of 99% at a specific energy consumption (SEC) of 10.34 kWh/kg COD. The results indicated that both current density and concentration of $FeSO_4$ have a major impact on the elimination of COD, while time has a minor effect. The adequacy of the model equation was demonstrated by its high R^2 value (0.987). The present work demonstrated that the graphite–graphite EF system could be considered as an effective approach for removing of COD from petroleum refinery wastewaters.

Keywords: advanced oxidation process; COD removal; electro-Fenton; porous graphite; response surface methodology.

INTRODUCTION

Petroleum refinery wastewaters (PRW) are considered as refractory wastewaters, which contain inorganic compounds as well as complex aromatics organic compounds (Diya'uddeen et al., 2011). The wastewaters generated from petroleum refinery processing have been recognized as highly toxic and relatively more refractory to natural degradation in comparison with other types of wastewaters that are generated from various industrial activities (Bayat et al., 2012). During the production stage in oil refinery processing, Coelho and his research group (Coelho et al., 2006) found that the amount of the used water be range from 0.4 to 1.6 times the volume of processed oil, hence causing serious damage to the environment. On the basis of the type of oil used, kind of processes, and the complexity of the refinery, the generated wastewaters in oil refineries may have different chemical compositions (Diya'uddeen et al., 2011, Zelmanov et al., 2005, Mrayyan et al., 2005). Generally, the COD values could be approximately 300–600 ppm; concentration of phenol in the range of 20–200 ppm; benzene in the range of 1–100 ppm; heavy metals such as lead (0.2–10 ppm); chromium (0.1–100 ppm) in addition to other pollutants are found in refinery effluent (World Bank Group, 1999). It is expected that the demand on global energy will be increased

to be 44% over the next two decades making the handling of petroleum refinery process and its generated wastewater are important issues, hence, innovative methods should be applied to remove these toxic pollutants (IPIECA, 2010).

Various traditional methods have been utilized for PRW treatment, namely, flocculation, coagulation, adsorption, biological process, membrane, and others (Augulyte et al., 2009, El-Naas et al., 2010). The most common industrial process is a biological one (Diya'uddeen et al., 2011). In these methods, contaminants are converted from one phase to another or partially degrading PRW; therefore, these approaches are not optimal. Advanced oxidation processes (AOPs) can quickly eliminate the non-biodegraded contaminants existing in the aquatic environment. Organic pollutants in wastewater can be removed with great efficiency by these processes, even when they are present in low concentrations without creating environmentally harmful byproducts (Catalkaya et al., 2009; Giri et al., 2014). Because of its ability to generate hydroxyl radicals in high concentrations, Fenton process is considered as one of the most AOPs commonly used in treatment of wastewater. Using Fenton process is restricted economically because of the high cost of H_2O_2, the huge amount of generated iron sludge, and its acidic pH requirements (Nidheesh et al., 2012).

Recently, electrochemical advanced oxidation processes (EAOPs) have received much attention for waste water treatment. They are based on Fenton's reaction chemistry and became ecofriendly approaches (Brillas et al., 2009). The most popular EAOPs is electro Fenton (EF) process (Zhang et al., 2009). In comparison with the traditional Fenton process, the EF process has the benefit of permitting superior process control, avoiding H_2O_2 storage or transportation, and no iron sludge generation (Cheng-Chun et al., 2007). In this method, the contaminated solution is furnished by H_2O_2 continuously via two electron oxygen reduction on a cathode of electrolytic cell in an acidic medium according to the following equation (Peralta-Hernández et al., 2006):

$$O_2 + 2H^+ + 2e^- \rightarrow H_2O_2 \quad (1)$$

Furthermore, electricity which is used in the EF process is considered as a clean energy source and the process as a whole does not produce secondary contaminants (Cheng-chun et al., 2007). The EF process is an environment friendly technique for treating wastewater since it does not use any dangerous reagents (Ghoneim et al., 2011). In the manufacturing of H_2O_2 based on Eq.(1), many carbon-based electrode have been used, including graphite (Wang et al., 2008), carbon sponge (Özcan et al., 2008), carbon fiber (Wang et al., 2005), vitreous carbon (Alverez et al., 2006.), and the gas diffusion electrode (Pozzo et al., 2005). Traditionally, electrochemical production of H_2O_2 has been achieved by using graphite due to its low cost (Wang et al., 2008).

EF depends on the catalytic electro generation of Fenton's reagent – a mixture of ferrous ions and H_2O_2 to yield hydroxyl radicals ($OH^{\bullet}$) which can destroy the toxic organic compounds in aqueous media (as equations 2–5) (Zhang et al., 2014).

$$H_2O_2 + Fe^{2+} \rightarrow Fe^{3+} + OH^- + OH^{\bullet} \quad (2)$$

$$RH + OH^{\bullet} \rightarrow R\bullet + H_2O \quad (3)$$

$$R\bullet + O_2 \rightarrow \text{products} \quad (4)$$

$$R\bullet + OH^{\bullet} \rightarrow \text{products} \quad (5)$$

For EF, the optimum pH is 3. The EF oxidation efficiency decreased at pH value higher than 3 as a result of generating low active $Fe(OH)_3$which has a lesser affinity to react with H_2O_2 while a pH value lower than 3 generates less hydroxyl radicals and increases the scavenging effect of H^+ and hydroxyl radicals (Mirshahghassemi et al., 2016).

For every electrochemical process, the design of an electrochemical reactor is a major difficulty. It necessitates an understanding of thermodynamics, kinetics, potential and current distribution, and flow configuration of electrolyte. A wide range of cell configurations, from open tanks to parallel-plate cells to sophisticated configurations with fluidized bed electrodes, are routinely utilized in the EF process. Dual-electrode electrochemical reactors are the simplest of these designs, with a lower potential drop than any of these cell types (Pletcher, 1990; Nidheesh et al., 2015). On the other hand, electrochemical reactors have many common features with conventional chemical reactors in terms of operation and characteristics. On the basis of flow configuration, electrochemical reactors can be divided into simple batch reactors, single-pass continuous stirred tank reactors, single-pass plug flow reactors, and batch recirculation modes. On the conducting fundamental research or developing commercial applications, many scientists have turned to the electrochemical reactor with batch recirculation

Table 1. Properties of the effluents generated by the Al-Dewaniya petroleum refinery plant

Property	COD (mg/l)	pH	Turbidity (NTU)	Conductivity (mS/cm)	T.D.S. (mg/l)	Phenol (mg/l)	SO^{-2}_4 (mg/l)	Cl^- (mg/l)
Raw effluent	2455	7.4	29.6	10.77	4267	14.2	126	2128

mode as a highly adaptable laboratory-scale reactor (Manivasagan et al., 2012). Few studies have stated that graphite can be utilized as anode and cathode in the EF process (Yang et al., 2012). (Nidheesh et al., 2014a) stated that removal of dyes by adopting graphite–graphite EF system is more efficient as an electrochemical system (Nidheesh et al., 2014b; Nidheesh et al., 2014c, Nidheesh et al., 2013). The same conclusion was drawn in the removal of salicylic acid from aqueous solution (George et al., 2013a; George et al., 2013b). The advantage of the graphite–graphite EF process as reported by (Nidheesh.et al., 2014b) is that using the graphite–graphite EF system will improve the effectiveness of the system as a result of forming graphite layer on the cathode from anode particles with no effect on the homogeneity of the system. Therefore, for the first time, a tubular electrochemical reactor was used as a new design which composed from cylindrical porous graphite as cathode and concentric porous graphite rod as anode for treatment petroleum refinery wastewater using batch recirculation mode of operation. To the best of authors' knowledge, no research reported the use of graphite–graphite EF system for treatment of petroleum refinery wastewater at batch recirculation mode of operation.

On the other hand, this work examined the viability and efficiency removal of COD from petroleum refinery wastewater using the EF technology in which H_2O_2 was in-situ produced at porous graphite cathode and Fe^{2+} was inserted externally. Constant-current mode was used to estimate the COD elimination efficiency, since it is more preferable for industrial scale-up. The Box-Behnken design (BBD) was adopted to study and optimize the influences of many operating parameters, including applied current density, concentration of $FeSO_4$, and time, on the removal of COD from wastewater produced by the Al-Dewaniya petroleum refinery plant.

EXPERIMENTAL WORK

At the Al-Dewaniya refinery plant, 14 liters of effluent from the feeding tank to the biological treatment unit was collected and stored in covered containers at 4 °C until usage. Table 1 provides a breakdown of the sample characteristics. There is no need for using supporting electrolyte, since the measured conductivity of wastewater was 10.77 $mScm^{-1}$, in accordance with the limit needed to achieve low cell voltage (Souza et al., 2013).

The electrochemical system under study composed of a cylindrical tank with capacity (1.25 L), an electrochemical reactor, a dosing pump (type-HYBL5LNPVF001, Italy) with maximum pressure of 10 bar and a flow rate of (1–3 L/h), a liquid flow meter (type-ZYIA, 25–250 ml/min, China), an air flow meter (0–5 l/min., China), and air pump (model-ACO-208, 45W, China). The acrylic cylindrical reservoir has dimensions (200 mm in height, outside diameter of 100 mm and thickness of 4 mm) having a cover with dimensions (outside diameter of 120 mm and thickness of 10 mm). The reservoir has two outlets one at its bottom and the other on its side located above its base at a distance of (30 mm). Each outlet was provided with a PVC valve. The cover was provided with three inlets; the first is for the recycle from the electrochemical reactor, the second is for the air coming from air pump for saturating the solution with oxygen and providing the mixing for solution, while the third is for feeding the solution. Figure 1 shows the schematic diagrams for the electrochemical system.

The electrochemical reactor which is the backbone of the electrochemical system is a new design adopted in the present work. It is made of transparent Acrylic material, Perspex type. It is composed of three compartments: upper, central, and bottom compartments. The bottom compartments serves as a feeding chamber for the reactor. It has a cylindrical shape with dimensions (outside diameter of 70 mm, total length of 50 mm, and thickness of 4 mm) ended at its upper face with a flange having dimensions (outside diameter of 100 mm and thickness of 10 mm) and contained four holes (5 mm in diameter) for fixing the compartment with the others via bolts and nets. The bottom compartment has two inlets having a diameter of 10 mm. The first for entering the solution is located at the side of compartment while

the second for entering air is located at the bottom of the compartment. The central compartment has a cylindrical shape with dimensions (outside diameter of 70 mm, total length of 70 mm, and thickness of 4 mm) ended at its upper and lower faces with flanges having dimensions (outside diameter of 100 mm and thickness of 10 mm) and each one contained four holes. A porous graphite cathode has dimensions (outside diameter 60 mm, thickness 5 mm and length of 55 mm) was fixed inside the central compartment via copper bolt at the midpoint of the lateral surface of the compartment. The internal geometric area of cathode was 81.54 cm^2, a value that was used for determining its current density. Upper flange was provided by perforated ring with the dimensions of (outside diameter of 68 mm, inside diameter of 20 mm, and thickness of 3 mm) made from the same material of the compartment, while the lower flange was provided with perforated disc having the dimensions of (outside diameter of 68 mm, and thickness of 3 mm). Both ring and disc were perforated uniformly with hole of 1 mm at equal distance among them. The upper compartment serves as a collecting chamber and as a holding for the anode. It has a cylindrical shape with the dimensions of (outside diameter of 70 mm, total length of 50 mm, and thickness of 4 mm) ended at its lower face with a flange having the dimensions of (outside diameter of 100 mm and thickness of 10 mm) and contained four holes. A porous graphite rode has dimensions (length of 107 mm and diameter of 28 mm) serves as anode and it was fixed inside the chamber via copper bolt at the center point of the upper base of the chamber. The distance between electrodes (anode and cathode) was fixed at 10 mm. Anode and cathode were made of porous graphite (Tokai Carbon Co., Ltd. provides a type UHP graphite electrode with a porosity of 20% to 26% for use in ARC furnaces.) and its BET surface area was 22.7509 m^2/g (Abbar et al., 2020). Figure 2 shows the schematic design of electrochemical reactor.

The chemicals used in the present study were analytical grade, $FeSO_4.7H_2O$ (purity 99.5%,

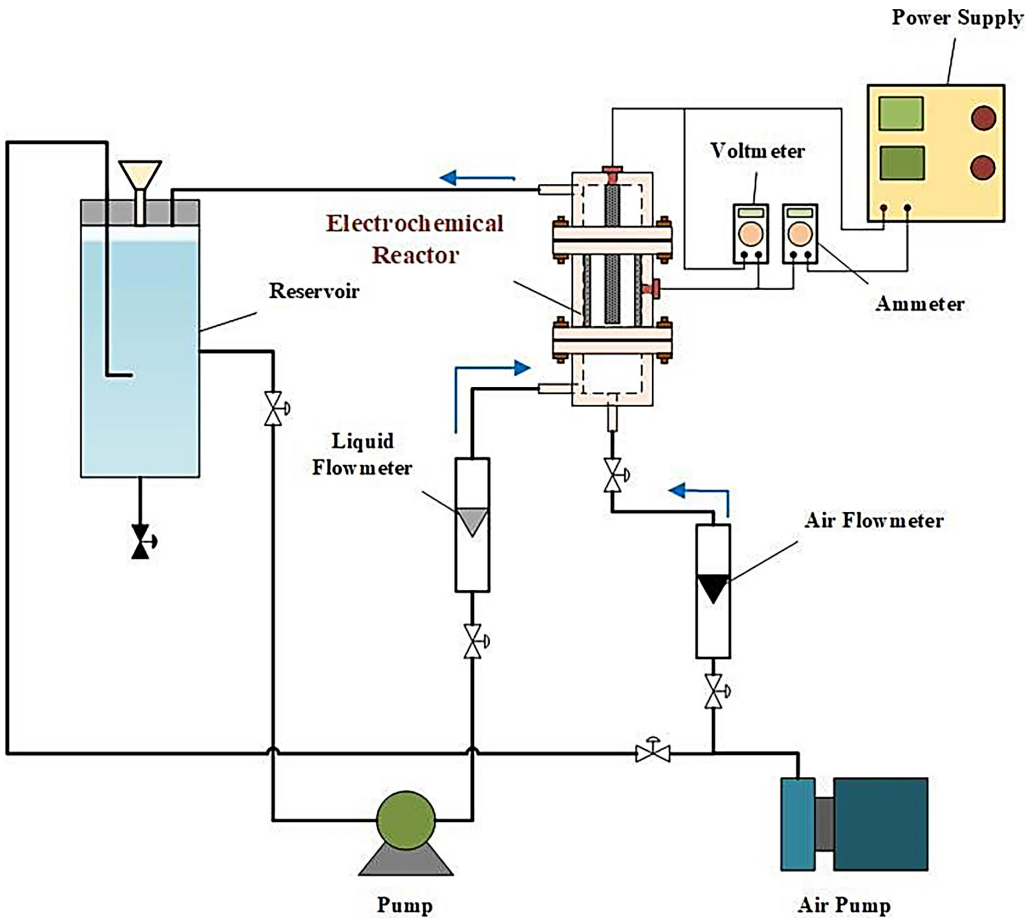

Figure 1. Schematic diagram of the electrochemical system

Thomas baker, India), H_2SO_4 (98%, Thomas baker, India) and NaOH (purity 99%, BDH, England).

Before starting each experiment, 1L of wastewater was taken and put inside 2 liter beaker mounted on a magnetic hot plate stirrer (Heidolph,MR Hei-standard, Germany). Its pH was firstly adjusted to 4 by adding 1M H_2SO_4 to make the iron species soluble then the required amount of $FeSO_4.7H_2O$ was added then the solution was homogenized for 15 min followed by adjusting its pH to 3 before using. The waste solution then placed in the feeding tank, then the dosing pump was turned on for circulating the solution through the electrochemical reactor for 15 minutes during this period air was bubbled in the solution to saturate it with oxygen and continue till the end of experiment. This continuous aeration maintains the saturated level of oxygen till the end of electrolysis. Liquid flow rate was adjusted to 200 ml/min and air flow rate to 3L/min. After that, a constant current was applied to the electrochemical reactor via D.C power supply (UNI-T, UTP3315TFL-II, China) and the electrolysis was continued for a period of time at a constant temperature of 25±2 °C.

At the end of each run and before carrying out COD tests, solution pH was adjusted to 8.0 for removing residual Fe^{2+}(Fe^{3+}) then filtrated and tested its COD value. A digital pH meter was used to measure the electrolyte pH (type - PH211, HNNA Instrument Inc. Romania). To measure the conductivity and the TDS, conductivity meter type COM-100, HM digital Inc. Korea was used. At the end of the electrolysis process, the samples were collected and examined to determine the levels of COD and phenol. Solution turbidity was measured by (Jenway-6035, Germany). SO_4^{-2} and Cl^{-1} was analyzed by using Photo Flex. Series, (WTW model no 14541, Germany).

COD is defined as the amount of a specified oxidant that reacts with the sample under controlled conditions. The level of COD in the effluent was used as a measure of the amount of organic compounds in the waste stream. The concentration of COD in the petroleum refinery effluents was evaluated by digesting 0.2 ml of effluent for 120 minutes at 150 °C using $K_2Cr_2O_7$ as an oxidizing agent in a thermo reactor (RD125, Lovibond). After cooling down the sample to room temperature, COD concentration was detected by spectrophotometer

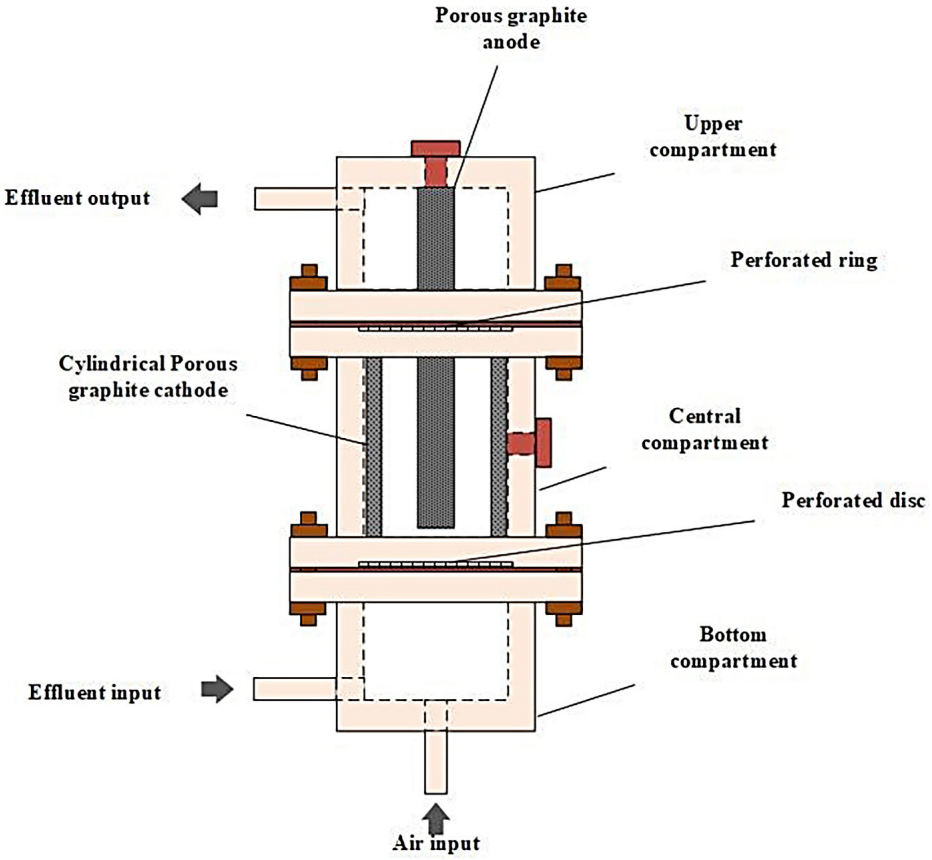

Figure 2. Schematic diagram of the electrochemical reactor

(MD200, Lovibond). Method 8047 of the Hach Company/Hach Lange GmbH, USA, was used to measure phenol. COD was measured three times, with the averages used in this study.

Evaluation of COD removal efficiency was performed using Eq. 6 (Abbar.et al., 2020).

$$RE\% = \frac{COD_i - COD_f}{COD_i} \times 100 \quad (6)$$

where: RE% – the removal efficiency, the initial COD (mg/L) represented by COD_i, and the final COD (mg/L) represented by COD_f.

When digesting a kilogram of COD, the specific energy consumption (SEC) is the total quantity of energy that is used. It is possible to calculate the SEC (kWh/kg) using Eq. 7 (Abbar.et al., 2020):

$$SEC = \frac{E.I.t \times 1000}{(COD_i - COD_f)\,V} \quad (7)$$

where: E denotes the applied cell potential in Volt, I denotes the current in ampere, t denotes the electrolysis duration in hours, and SEC denotes specific energy consumption (kWh/kg COD).

Design of experiments

RSM is summarized as a group of mathematical and statistical tools for determining a regression model equation that correlate an objective function with its independent variables (Bezerra et al., 2008). The 3-level 3-factor Box–Behnken design (BBD) was adopted to examine the impact of process variables on COD removal. The removal effectiveness of COD (RE percent) was taken into account as a response, while the current density (X1), Fe SO_4 concentration (X2), and time (X3) were taken into account as process parameters (El-Ghenymy et al., 2008). The scales of process components were labeled as low (-1), middle or centre point (0), and high level (1). Table 2 shows the process factors with their selected levels while Table 3 shows the experiments array provided by BBD for the current work, which was obtained by the Minitab-17 program.

In this work, the relationship between the response and their independent variables was obtained by the following second-order model with a least-squares method (El-Ghenymy et al., 2008):

Table 2. Coded and real levels of the process parameters in the refinery wastewater treatment

Process parameters	Range in Box–Behnken design		
Coded levels	Low(-1)	Middle (0)	High (+1)
Current density (mA/cm^2), X1	5	15	25
Concentration of Fe SO_4(mM), X2	0.2	0.8	1.4
Time(min), X3	30	60	90

Table 3. Experimental design array based on Box-Behnken

Run order	Blocks	Coded value			Real value		
		x_1	x_2	x_3	Current density (mA/cm^2), *X*1	$FeSO_4$ (mM), *X*2	Time (min.), *X*3
1	1	0	1	1	15	1.4	90
2	1	-1	1	0	5	1.4	60
3	1	1	1	0	25	1.4	60
4	1	-1	-1	0	5	0.2	60
5	1	-1	0	1	5	0.8	90
6	1	0	-1	1	15	0.2	90
7	1	1	0	1	25	0.8	90
8	1	1	0	-1	25	0.8	30
9	1	0	0	0	15	0.8	60
10	1	0	0	0	15	0.8	60
11	1	0	-1	-1	15	0.2	30
12	1	-1	0	-1	5	0.8	30
13	1	1	-1	0	25	0.2	60
14	1	0	0	0	15	0.8	60
15	1	0	1	-1	15	1.4	30

$$Y = a_0 + \sum a_i x_i + \\ + \sum a_{ii} x_i^2 + \sum a_{ij} x_i x_j \quad (8)$$

where: a_0 symbolises intercept term, *j* and *i* symbolise the index numbers for patterns, a_i symbolises the first-order (linear) main effect, a_{ii} symbolises second-order main effect and a_{ij} symbolises the interaction effect, x_1, x_2, … x_k denote the process factors in coded form and finally *Y* denotes the response (RE%).

Analysis of variance (ANOVA) was achieved then the confirmation of model adequacy was achieved by calculating the regression coefficient (R^2).

RESULTS AND DISCUSSION

Results of experimental design

According to the BBD design, fifteen runs were performed to investigate the optimum conditions for COD removal. Table 4 displays the experimental results involving the efficiency of COD removal (RE%) and specific energy consumption (SEC).

The results showed that efficiency of COD removal was in the range of 82–95.67% while the specific energy consumption ranged between 0.4 kWh/kg COD and 10.92 kWh/kg COD. It is clear that adopting BBD gave better combination of process variables for obtaining COD removal higher than 80%. As a preliminary inspection, a comparison between run (3) and run (4) showed that the concentration of $FeSO_4$ has a major impact on the removal efficiency of COD where RE% increased from 82 to 95.67% making a difference of 13.67% as $FeSO_4$ concentration increased from 0.2 to 1.4 mM at constant current density of 25 mA/cm^2 and time of 60 min., while the comparison between run (2) and run (3) showed that current density followed the $FeSO_4$ concentration in his effect on the COD removal efficiency where RE% increased from 88.43 to 95.67% making a difference of 7.24% as the current density increased from 5 to 25 mA/cm^2 at constant $FeSO_4$ concentration of 1.4 mM and time of 60min. However, the precise effect of these parameters can be observed via the ANOVA results.

By using Minitab-17 software, A quadratic model of the removal effectiveness of COD (RE percent) in terms of real units of process parameters was developed using the results of the analysis:

$$RE\% = 85.16 + 0.096\ X1 + 5.29\ X2 - 0.1533\ X3 + \\ 0.00570\ (X1)^2 - 3.89\ (X2)^2 + 0.000913\ (X3)^2 + \\ + 0.0850\ X1 \cdot X2 + 0.00020\ X1 \cdot X3 + \\ + 0.0886\ X2 \cdot X3 \quad (9)$$

Here, the interaction effect of model parameters is depicted as X1X2, X1X3, and X2X3. The measuring of the major influence of model

Table 4. Experimental results of COD removal using Box–Behnken design

Run order	*X*1	*X*2	*X*3	*E* (V)	COD (ppm)		RE%		SEC ($\frac{KWh}{kg\ COD}$)
					Initial	Final	Actual	Predicted	
1	15	1.4	90	6.25	2395	146	93.90	94.47	5.04
2	5	1.4	60	3.94	2420	280	88.43	87.74	0.73
3	25	1.4	60	8.44	2425	105	95.67	95.69	7.56
4	5	0.2	60	3.96	2390	430	82.00	81.98	0.80
5	5	0.8	90	3.90	2450	299	87.79	87.92	1.08
6	15	0.2	90	6.26	2467	380	84.59	84.49	5.55
7	25	0.8	90	8.65	2480	110	95.56	94.98	10.92
8	25	0.8	30	8.95	2420	165	93.18	93.05	4.06
9	15	0.8	60	6.38	2430	275	88.68	89.16	3.56
10	15	0.8	60	6.89	2380	246	89.66	89.16	3.93
11	15	0.2	30	7.00	2397	325	86.44	85.88	2.08
12	5	0.8	30	4.14	2369	340	85.65	86.24	0.40
13	25	0.2	60	9.00	2400	307	87.20	87.89	8.96
14	15	0.8	60	6.50	2436	265	89.12	89.16	3.63
15	15	1.4	30	6.30	2398	255	89.37	89.47	1.79

parameters are represented by their double effect $(X1)^2$, $(X2)^2$ and $(X3)^2$. Table 4 shows the estimated COD removal efficiency values based on Equation 9. In Eq. 9, the positive coefficient in front of any parameter reveals that RE% increases with its increasing and vice versa.

Analysis of variance (ANOVA) was used to determine the acceptability of BBD. Fisher's F-test and P-test are analytical tools used to determine the significance of the model and its parameters (Segurola et al., 1999). Larger F-values and smaller p-values are often seen as more significant coefficient terms (Arunachalam et al., 2011). The response surface model's ANOVA results are shown in Table 5. The contribution of each variable is represented by its percentage, DF indicates the degree of freedom of the model and its parameters. Seq. SS, Adj. SS, and Adj. MS imply statistical terms of ANOVA. On the basis of results, the regression model has a P-value of (0.0001) and an F-value of (43.02). Regression was shown to be statistically significant with a multiple correlation coefficient of 0.9872, with only (0.0128) of the total variation not supported by the model. Since the difference between adj. R^2 (0.9643) and pred. R^2 (0.8260) is smaller than 0.2, they are well-matched (Zhao et al., 2011).

The results of Table 5 showed that both $FeSO_4$ concentration and current density have the major effect with contributions of 43.59% and 41.71% respectively. In turn, time has the lower effect of 2.95%.

The approximated contributions of current density and $FeSO_4$ concentration confirm that EF governed by these two variables at the same degree. This result is expected, since the EF process is governed by Eq. 2 in which Fe^{+2} is furnished externally by adding $FeSO_4$ and H_2O_2 is generated internally by applying current density. The squared interactions are not significant, except for the double effect of Fe concentration.

The 2-way interactions among the variables are non-significant accept the interaction between time and current density. The P-value for lack-of-fit (0.246) is higher than 0.05 in the present investigation, confirming that the lack of model fit was not statistically significant compared to the pure error. As a result, the model can accurately predict the response levels. The contribution of linear term was 88.26%, while the square and 2-way interaction were 5.33% and 5.09%, respectively. Hence, the overall interaction effect is significant.

Influence of process parameters on the efficiency of COD removal

The graphical representations of RSM can be used to illustrate interactive effects of the selected

Table 5. Analysis of variance for COD removal

Source	DF	Seq. ss	Contr.%	Adj. ss	Adj. Ms	F-value	P-value
Model	9	217.832	98.72	217.832	24.2036	43.02	0.0001
Linear	3	194.740	88.26	194.740	64.9133	115.37	0.0001
(*X*1)	1	96.188	43.59	96.188	96.1884	170.95	0.0001
(*X*2)	1	92.032	41.71	92.032	92.0317	163.57	0.0001
(*X*3)	1	6.520	2.95	6.520	6.5197	11.59	0.019
Square	3	11.856	5.37	11.856	3.9519	7.02	0.030
*X*1*X1	1	1.397	0.63	1.201	1.2007	2.13	0.204
*X*2*X2	1	7.966	3.61	7.250	7.2499	12.89	0.016
*X*3*X3	1	2.493	1.13	2.493	2.4933	4.43	0.089
2-Way Inter.	3	11.237	5.09	11.237	3.7456	6.66	0.034
*X*1*X2	1	1.040	0.47	1.040	1.0404	1.85	0.232
*X*1*X3	1	0.014	0.01	0.014	0.0139	0.02	0.881
*X*2*X3	1	10.182	4.61	10.182	10.1825	18.10	0.008
Error	5	2.813	1.28	2.813	0.5627		
Lack of Fit	3	2.331	1.06	2.331	0.7771	3.22	0.246
Pure-Error	2	0.482	0.22	0.482	0.2410		
Total	14	220.65	100				
Model-summary		*S*.	R^2	R^2(adj.)	PRESS	R^2 (pred.)	
		0.75013	98.72%	96.43%	38.3858	82.60%	

variables and their effect on the response. For different values of current density (5–25 mA/cm^2) and constant time of 60 min, the influence that the $FeSO_4$ concentration has on the RE percentage can be observed as shown in Figures (3a, b). The response surface plot is depicted in Figure 3a, while the contour plot presented in Figure 3b. The form of control plot reveals the type and magnitude of the interaction between variables. At a current density of 5 mA/cm^2, an improvement in the COD removal efficiency can be seen as the $FeSO_4$ concentration rises from 0.2 to 1.4 mM as shown in Figure 3a. The increasing in RE% occurs rapidly at the first stage then tends to be sluggish at the end. A Similar observation was made at higher current density (25 mA/cm^2). This behavior can be interpreted as increasing Fe^{+2} concentration improved the H_2O_2 oxidizing power for destroying large molecules; therefore, increasing the concentration of Fe^{+2} leads to more degradation of organic compounds in wastewater (Ahmadi et al., 2020, Huanqi et al., 2017). Previous studies showed that Fe^{+2} has the ability to destroyed large molecule in wastewater such as dyestuffs in real dyeing wastewater (Wang et al., 2010). At any concentration of $FeSO_4$, RE% increases linearly with increasing current density from 5 to 25 mA/cm^2. This behavior of the effect of current density on RE% is also observed in previous works (Sahraei et al., 2013; Davarnejad et al., 2015) and could be explained as the current is considered the driving force for the reduction of oxygen on the cathode surface leading to generate H_2O_2; hence, by increasing the current density, greater generation of $OH^{\bullet}$ would happened due to the reaction of H_2O_2 with ferrous ions. On the contour plot, it can be seen that the COD removal effectiveness of over 95% lies within an extremely narrow band of current density (22–25 mA/cm^2) and $FeSO_4$ concentration between (0.9–1.4 mM).

For various current densities (5–25 mA/cm^2) and at constant $FeSO_4$ concentration (0.8 mM), the effect of time on the RE percent is shown in Figures (4a, b). The COD removal efficiency increases exponentially with increasing time at all current density, as shown in Figure 4a. According to the previous studies (Davarnejad et al., 2015, Fathinejad Jirandehi et al., 2015, Adimi et al., 2017, Yan et al., 2014), these findings are in line with previous findings. Reaction time has a favorable impact on the electro-Fenton process, according to the data. It is clear from the contour plot Fig. 4b that a region with a current density of 24–25 mA/cm^2 and time ranging from 80–90 minutes is responsible for the COD elimination effectiveness of 95 percent. In other words, using RSM will reveal the optimal ranges of parameters and the ways in which the factors interact with each other.

The optimum operating conditions with confirmation test

In order to reduce energy waste, electrochemical systems must be optimized. In order to maximize the desirability function (D_F) and achieve the intended outcome, various criteria must be recognized during the optimization process (Bezerra et al., 2008). Minimize, Maximize, objective, within the range, and none are all regarded as alternatives for the target function. Removal of COD was intended to remove as much as possible, and this was done by setting D_F = 1.0 as the target removal goal. The process variables

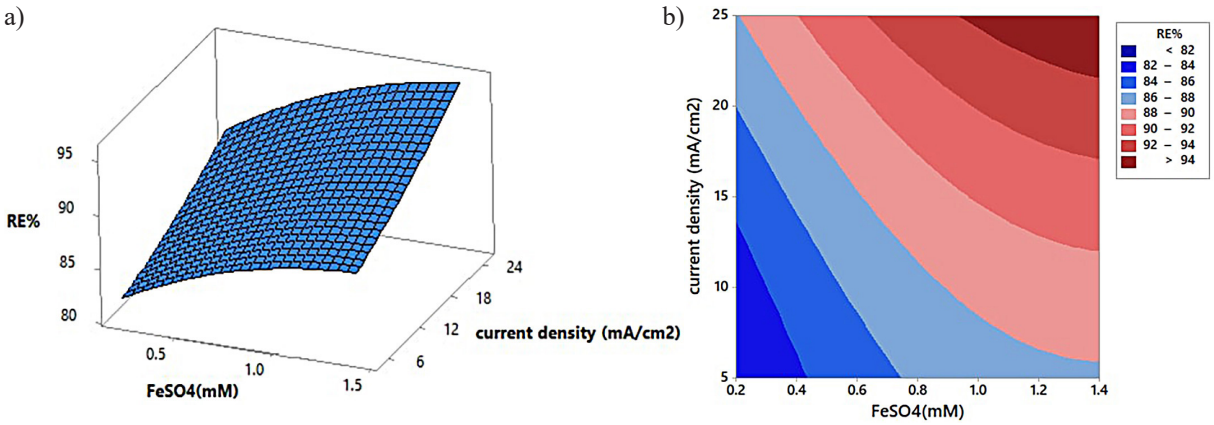

Figure 3. Impact of $FeSO_4$ concentration and current density on the RE%; a) response surface plot, b) contour plot (Hold values: time = 60 min)

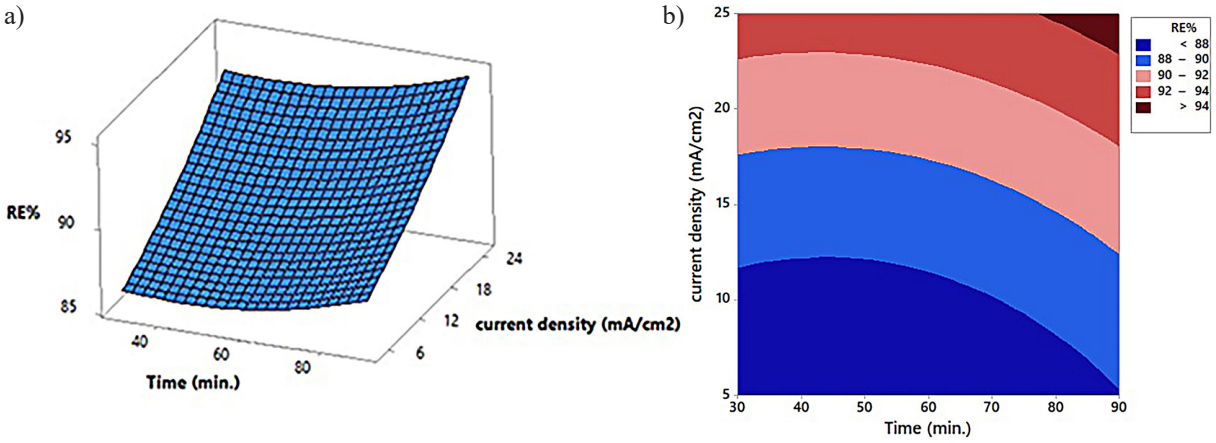

Figure 4. Impact of time and current density on the RE%; a) response surface plot, b) contour plot; (Hold value: FeSO4 concentration = 0.8 mM)

evaluated in this paper were current (from 5 to 25 mA/cm^2), $FeSO_4$ concentration (from 0.2 to 1.4 mM), and duration (from 30 to 90 minutes). The highest limit was set at 95.69 percent, while the lower limit for COD removal efficiency was set at 82 percent. Table 6 shows the outcomes of optimization under these parameters and settings. Using the adjusted settings, two more confirmatory tests were run, as shown in Table 7. At pH = 3, an average of 98.93 percent COD removal was accomplished after 90 minutes of electrolysis, which falls within the range of optimum values determined by optimization study (Table 6). As a result, using BBD in conjunction with porous graphite–graphite EF systems is successful and effective in optimizing the removal of COD. The comparison of effluent parameters between treated and untreated wastewater is shown in Table 8. In this study, it was observed that the treated wastewater has superior qualities and complies with the standard limits for effluent discharge (100 ppm). The activity of the EF process using the new design of electrochemical reactor in the treatment of the wastewater generated from the Al-Dewaniya petroleum refinery plant was approved in this study, where a COD removal efficiency of 99.02 percent was obtained in combination with phenol removal efficiency of 96.3

Table 6. Maximizing of COD removal efficiency (RE%) with its optimal process parameters

Response	Goal	Lower	Target	Upper	Weight	Importance
RE (%)	Maximum	82	Maximum	95.69	1	1
Solution: parameters			Results			
Current density (mA/cm^2)	$FeSO_4$ (mM)	Time (min)	RE (%) Fit	D_F	SE Fit	95% CI	95% PI
25	1.4	90	99.0733	1	0.886	(96.795,101.351)	(96.089,102.058)

Table 7. Confirmative value of the optimum COD removal efficiency

Run	Current density (mA/cm^2)	$FeSO_4$ (mM)	Time (min)	E (Volt)	COD (ppm)		RE (%)		EC (Kwh/kgCOD)
					Initial	Final	Actual	Average	
1	25	1.4	90	8.26	2455	24	99.02	98.93	10.34
2	25	1.4	90	8.28	2468	28.3	98.85		10.31

Table 8. Properties of the treated effluent and raw effluent

Parameter effluent	COD (ppm)	Phenol (ppm)	Turbidity (NTU)	SO_4^{-2} (ppm)	Cl^- (g/l)
Raw effluent	2455	14.2	29.6	126	2.128
Treated effluent	24(99.02%)	0.525(96.3%)	0.885(97.01%)	712	1.963

percent, and turbidity removal efficiency of 97.01 percent. The sulfate ions in the treated effluent have increased due to the use of ferrous sulphate, whereas chlorine ions have decreased as a result of producing of chlorine on the anode.

The results of the present work reveal that the graphite–graphite EF system can be applied successfully for treatment of the Al-Dewaniya petroleum refinery. Starting from an initial COD of 2455 ppm, a COD removal efficiency of 99% it could be achieved at 90 min with an energy consumption not exceeded 10.34 kWh/kg COD. These results prove that the EF process has the ability to oxidize the refractory natural or organic compounds that exist in petroleum refinery wastewater in a more proficient way.

In the literature, most studies that adopted the graphite–graphite EF system were conducted in batch mode of operation. No previous works using the graphite–graphite EF system were conducted in batch recirculation mode, so the authors were unable to make a comparison with them. However, in comparison with the previous works that used the graphite–graphite EF system (Nidheesh et al., 2014b, George. et al., 2013) in batch mode, the present system required less time with reaching high removal efficiency which is an indication on the importance of the recirculation for increasing mass transfer, leading to higher removal with lower electrolysis time. Moreover, the present system could be considered as an economic one since it used electrodes made from cheap materials and its specific energy consumption is approximately lower and suitable in comparison with previous studies (Abbar et al., 2020).

CONCLUSIONS

This research focused on the removal of COD from petroleum refinery wastewater by graphite–graphite EF system operated in batch recirculation mode. The response surface approach was used to conduct experiments to determine the influence of current density, $FeSO_4$ concentration, and time on the reduction of COD in petroleum refinery effluent generated at the Al-Dewaniya refinery plant in Iraq. The refinery. On the basis of BBD, the best conditions were achieved at a current density of 25 mA/cm^2, a $FeSO_4$ concentration of 1.4 mM, and a time of 90 minutes, in which COD removal and specific energy consumption were 99% and 10.34 kWh/kg, respectively. The high R^2, adj. R^2 and pred. The R^2 value indicates that the model fitted very well to the experiment data; besides, the results indicate that RSM can be successfully used to analyzing the impact of various operating factors and developing the required optimum conditions, thus reducing the number of runs, time, and cost of experiments.

The efficiency of the graphite–graphite EF system was found to depend on two main parameters (current density and $FeSO_4$ concentration) at approximately the same contribution of their effect on COD removal. Time was found to have the least effect. It is obvious that the batch recirculation mode was able to operate the system without operational problems, and achieved good COD removal during a circulation time of 90 min. From present work, graphite–graphite EF system appears to be an environmentally friendly method to decrease the level of COD from petroleum refinery wastewater.

Acknowledgments

Thanks for the employees of Chemical Engineering Department at College of Engineering, University of Al-Qadisiyah for their technical assistance, the authors have been able to complete this study.

REFERENCES

1. Abbar A., Fahim A. 2020. Treatment of petroleum refinery wastewater by electro-Fenton process using porous graphite electrodes. Egyptian Journal of Chemistry, 63(12), 4805–4819. DOI: 10.21608/ejchem.2020.28148.2592
2. Adimi M., Mohammad Pour M., Fathinejad Jirandehi H. 2017. Treatment of Petrochemical wastewater by Modified electro - Fenton Method with Nano Porous Aluminum Electrode. J. Water Environ. Nanotechnol., 2(3), 186–194.
3. Ahmadi E., Shokri B., Mesdaghinia A., Nabizadeh R., Reza Khani M., Yousefzadeh S., Salehi M., Yaghmaeian K. 2020. Synergistic effects of α-Fe2O3-TiO2 and Na2S2O8 on the performance of a non-thermal plasma reactor as a novel catalytic oxidation process for dimethyl phthalate degradation, Sep. Purif. Technol., 250, 117185.
4. Alverez-Gallegos A., Pletcher D. 1999. Electrochemical Treatment of Wastewater containing polyaromatic organic pollutants, Electrochemi. Acta, 44, 2483–2492.

5. Arunachalam R., Annadurai G. 2011. Optimized Response Surface Methodology for Adsorption of Dyestuff from Aqueous Solution. Environ J., Sci. Technol., 4(1), 65–72.
6. Augulyte L., Kliaugaite D., Racys V., et al. 2009. Multivariate analysis of a biologically activated carbon (BAC) system and its efficiency for removing PAHs and aliphatic hydrocarbons from wastewater polluted with petroleum products. Journal of Hazardous Materials, 170(1), 103–110.
7. Bayat M., Sohrabi M., Royaee S.J. 2012. Degradation of phenol by heterogeneous Fenton reaction using Fe/clinoptilolite. Journal of Industrial and Engineering Chemistry, 18(3), 957–962.
8. Bezerra M.A., Santelli R.E., Oliveira E.P., Villar L.S., Escaleira L.A. 2008. Response Surface Methodology (RSM) as a Tool for Optimization in Analytical Chemistry, Talanta, 76(5), 965–977.
9. Brillas E., Sires I., Oturan M.A. 2009. Electro-Fenton process and related electrochemical technologies based on Fenton's reaction chemistry. Chem. Rev., 109, 6570–6631.
10. Catalkaya E.C., Kargi F. 2009. Advanced oxidation and mineralization of simazine using Fenton's reagent. Journal of Hazardous Materials, 168(2–3), 688–694.
11. Cheng-chun J., Jia-fa Z. 2007. Progress and prospect in electro-Fenton process for wastewater treatment, J. Zhejiang Univ. Sci. A, 8(7), 1118–1125.
12. Coelho A., Castro A.V., Dezotti M., Sant'Anna Jr G.L. 2006. Treatment of petroleum refinery sourwater by advanced oxidation processes. Elsevier Journal of Hazardous Materials, 137(1), 178–184.
13. Davarnejad R., Sahraei A. 2015. Industrial wastewater treatment using an electrochemical technique: an optimized process. Desalination and Water Treatment, 57(21), 9622–9634.
14. Davarnejad, R., Pirhadi, M., Mohammadi, M., Arpanahzadeh, S. 2015. Numerical Analysis of Petroleum Refinery Wastewater Treatment Using Electro-Fenton Process. Chem. Prod. Process Model, 10(1), 11–16.
15. Diya'uddeen B.H., Daud W.M.A.W., Abdul Aziz A.R. 2011. Treatment technologies for petroleum refinery effluents: a review. Process Safety and Environmental Protection, 89(2), 95–105.
16. El-Ghenymy A., Garcia-Segura S., Rodríguez R.M., Brillas E., El Begrani M.S., Abdelouahid B.A. 2012. Optimization of the electro-Fenton and solar photoelectron - Fenton treatments of sulfanilic acid solutions using a pre-pilot flow plant by response surface methodology. J. Hazard. Mater., 221–222, 288–297.
17. El-Naas M.H., Al-Zuhair S., Alhaija M.A. 2010. Reduction of COD in refinery wastewater through adsorption on date-pit activated carbon. Journal of Hazardous Materials, 173(1–3), 750–757.
18. Fathinejad Jirandehi H., Adimi M., Mohebbizadeh M. 2015. Petrochemical wastewater treatment by modified electro-Fenton process with nano iron particles. Journal of Particle Science & Technology, 1(4), 215–223.
19. George S.J., Gandhimathi R., Nidheesh P.V., Ramesh S.T. 2013a. Electro-Fenton method oxidation of salicylic acid in aqueous solution with graphite electrodes. Environ. Eng. Sci., 30, 750–756.
20. George S.J., Gandhimathi R., Nidheesh P.V., Ramesh S.T. 2013b. Electro-Fenton oxidation of salicylic acid from aqueous solution: batch studies and degradation pathway, Clean Soil Air Water, http://dx.doi.org/10.1002/clen.201300453.
21. Ghoneim M.M., El-Desoky H.S., Zidan N.M. 2011. Electro-Fenton oxidation of Sunset Yellow FCF azo-dye in aqueous solutions, Desalination 274, 22–30.
22. Giri A.S., Golder A.K. 2014. Fenton, photo-Fenton, H_2O_2 photolysis, and TiO_2 photocatalysisfor Dipyrone oxidation: Drug Removal, mineralization, biodegradability, and degradation mechanism. Industrial & Engineering Chemistry Research, 53(4), 1351–1358.
23. Huanqi H., Zhi Z. 2017. Electro-Fenton process for water and wastewater treatment. Critical Reviews in Environmental Science and Technology, 47(21), 1–32.
24. IPIECA (International Petroleum Industry Environmental Conservation Association) (2010) Petroleum refining water/wastewater use and management‖. Operations Best Practice Series, London, UK.
25. Manivasagan, V., Basha C.A., Kannadasan T., Saranya K. 2012. Degradation of Parachlorophenol by Electro-Fenton and Photo-Fenton Process Using Batch Recirculation Reactor. Portugaliae Electrochimica Acta, 30, 385–393.
26. Mirshahghassemi S., Aminzadeh B., Torabian A., Afshinnia K. 2016. Optimizing electrocoagulation and electro-Fenton process for treating car wash wastewater Environmental Health Engineering and Management, 4, 37–43.
27. Mrayyan B., Battikhi M.N. 2005. Biodegradation of Total Organic Carbons (TOC) in Jordanian Petroleum Sludge. J. Hazard Mater., 120(1–3), 127–134.
28. Nidheesh P.V., Gandhimathi R. 2013. Comparative removal of rhodamine b from aqueous solution by electro Fenton and electro Fenton like processes, Clean–Soil Air Water. http://dx.doi.org/10.1002/clen.201300093
29. Nidheesh P.V., Gandhimathi R. 2014b. Removal of Rhodamine B from aqueous solution using graphite–graphite electro-Fenton system. Desalination Water Treat., 52, 1872–1877.
30. Nidheesh P.V., Gandhimathi R. 2012. Trends in electro-Fenton process for water and wastewater treatment: an overview. Desalination, 299, 1–15.

31. Nidheesh P.V., Gandhimathi R., Velmathi S., Sanjini N.S. 2014c. Magnetite as a heterogeneous electro Fenton catalyst for the removal of Rhodamine B from aqueous solution, RSC Adv. 4, 5698–5708.
32. Nidheesh P.V., Gandhimathi R. 2015. Textile Wastewater Treatment by Electro-Fenton Process in Batch and Continuous Modes. Journal of Hazardous, Toxic, and Radioactive Waste, 19(3), 04014038.
33. Nidheesh, P.V., Gandhimathi R., Sanjini N.S. 2014a. NaHCO3 enhanced Rhodamine B removal from aqueous solution by graphite–graphite electro Fenton system. Separation and Purification Technology, 132, 568–576.
34. Özcan A., Şahin Y., Koparal A.S., Oturan M.A. 2008. Carbon sponge as a new cathode material for the electro-Fenton process: Comparison with carbon felt cathode and application to degradation of synthetic dye basic blue 3 in aqueous medium. J. Electroanal Chem., 616(1–2), 71–78.
35. Paz D.S., Foletto E.L., Bertuol D.A., Jahn S.L., Collazzo G.C., Silva S.S., Nascimento C.A. O. 2013. CuO/ZnO coupled oxide films obtained by the electro-deposition technique and its photocalyticactivity in phenol degradation under solar irradiation. Water Science and Technology, 68(5), 1031–1036.
36. Peralta-Hernández J.M., Meas-Vong Y., Rodríguez F.J., Chapman T.W., Maldonado M.I., Godínez L.A. 2006. In situ electrochemical and photo-electrochemical generation of the Fenton reagent: a potentially important new water treatment technology, Water Res. 40, 1754–1762.
37. Pletcher D., Walsh F.C. 1990. Industrial electrochemistry. Chapman & Hall, London.
38. Pozzo A.D., L.D.P., Merli C., Petrucci E. 2005. J. Appl Electrochem. 35, 413–419.
39. Sahraei A. 2013. Wastewater treatment obtained from the Imam Khomein's refinery using electro-Fenton technique. MSc Thesis: Arak University.
40. Segurola J., Allen N.S., Edge M., Mahon A.M. 1999. Prog. Org. Coat., 37, 23.
41. Silva S.S., Chiavone-Filho O., Neto E.L.B., Foletto E.L. 2015. Oil removal from produced water by conjugation of flotation and photo-Fenton processes. Journal of Environmental Management, 147, 257–263.
42. Souza R.B.A., Ruotolo L.A.M. 2013. Electrochemical treatment of oil refinery effluent using boron-doped diamond anodes. Journal of Environmental Chemical Engineering, 1(3), 544–551.
43. Wang A., Qu J., Ru J., Liu H., Ge J. 2005. Mineralization of an azo dye Acid Red 14 by electro-Fenton's reagent using an activated carbon fiber cathode Dyes Pigm., 65(3), 227–233.
44. Wang C.T., Hu J.L., Chou W.L., Kuo Y.M. 2008. Removal of color from real dyeing wastewater by Electro-Fenton technology using a three-dimensional graphite cathode. J. Hazard. Mater., 152, 601–606.
45. Wang C., Chou W., Chung M., Kuo Y. 2010. COD removal from real dyeing wastewaterby electro-Fenton technology using an activated carbon fiber cathode. Desalination, 253,129–134.
46. WBG (World Bank Group). 1999. Pollution Prevention and Abatement Handbook: Toward Cleaner Production, Washington, D.C., USA.
47. Yan L., Wang Y., Li J., Ma H., Liu H., Li T., Zhang Y. 2014. Comparative study of different electrochemical methods for petroleum refinery wastewater treatment. Desalination, 341, 87–93.
48. Yang C., Liu H., Luo S., Chen X., He H. 2012. Performance of modified electro-Fenton process for phenol degradation using bipolar graphite electrodes and activated carbon. J. Environ. Eng., 6, 613–619.
49. Zelmanov G., Semiat R. 2008. Phenol oxidation kinetics in water solution using iron(3)-oxide-based nano-catalysts. Water Research, 42(14), 3848–3856.
50. Zhang J., Shao M.H., Dong H. 2014. Degradation of Oil Pollution in Seawater by Bipolar Electro-Fenton Process. Polish Journal of Environmental Studies, 23, 933–941.
51. Zhang Li Z., Ai L. 2009. Design of a neutral electro-Fenton system with Fe@Fe2O3/-ACF composite cathode for wastewater treatment, J. Hazard. Mater. 164, 18–25.
52. Zhao Q., Kennedy J.F., Wang X.,Yuan X., Zhao B., Peng Y., Huang Y. 2011. Optimization of ultrasonic circulating extraction of polysaccharides from Asparagus officinal is using response surface methodology. Int. J. Biological Macromolecules, 49(2), 181–187.